Damping in Partially Delaminated Composites

Jong Hee Yim* and Bor Z. Jang**

(*Received March 10, 1997*)

A simple model was developed to predict the material damping in partially delaminated composites. First, we evaluated the damping loss factors experimentally in three kinds of specimens corresponding to various partial delamination areas. Second, the stiffness loss with delamination growth was assumed to result directly in the loss of energy from the oscillatory system because the delamination due to interlaminar stresses is accompanied with stiffness loss in numerous laminated composites. By correlating the laminate stiffness reduction and the corresponding delamination area, a model for their basic material damping properties was formulated using the elastic-viscoelastic principle, the rule-of-mixtures law and modified Hashin's Model. We predicted the damping of any partially delaminated composites with different stacking sequences based on Adams and Ni's work and their basic damping loss factors. Numerical and experimental results demonstrate that damping is significantly influenced by the size of delamination area in laminated composites. In addition, experimental improvements in making accurate damping measurements are discussed as well.

Key Words: Partial Delamination, Damping, Loss Factors, Random Vibration, Free-Free Support Condition, Laminated Composites

1. Introduction

The amount of deformation or damage experienced by a structure may be quantified by damping properties. The vibrational reponse of a lightly damped structure takes longer to decay than that of a heavily damped structure (Hashin, 1970; Adams, 1987). The structure responds with characteristic natural frequency and damping properties. Some structures exhibit numerous natural frequencies. Each natural frequency represents a particular pattern of deformation in the structure. These frequencies must be identified and separated for theoretical analysis. Damage may enhance the mechanical vibration damping for analysis, but obviously it deleteriously reduces the mechanical properties of the structure such as stiffness. Under static or fatigue loading, the damage mechanism of laminated composites exhibits progressive and cumulative damage, with matrix cracking preceding fiber breaks. The damage mechanisms in a composite are generally characterized as matrix cracking, delamination, fiber pull-out, fiber breakage, fiber/matrix debonding or various combinations of these five mechanisms. One matrix dominated form of damage is delamination cracks which are frequently found near the free edge of a laminate. Also, the degree of delamination damage frequently increases steadily until failure occurs by fiber fracture in the primary load carrying plies (Reifsnider et al., 1979). The delamination is found to depend strongly on laminate construction and stacking sequence. In laminated composites, stiffness reduction (Highsmith and Reifsnider, 1982; O' Brien, 1982) may be significantly influenced by delamination growth. In addition, the rate of stiffness loss with delamination growth can be related directly to dissipated strain energy rates.

We conducted an analysis to correlate the

* Kwangju-Chonnam Regional Small & Medium Business Office, Kwangju 502-200, Korea

** Dept. of Mechanical and Materials Engineering, Auburn University, Auburn, Alabama 36849, USA.

damping loss and stiffness reduction due to delamination size. Measurements of loss factors can be used to detect degradation in composite laminates based on correlation with other mechanical properties, and to develop monitoring models. The objective of this paper is to develop a reliable and effective method for predicting loss factor in partially delaminated composites and an improved experimental method.

Owing to extraneous energy dissipation, the damping values measured in the experiments were always greater than the true material damping. To significantly reduce the energy loss from the boundary, an experimental method proposed by Crocker and coworkers (Crocker et al., 1989) was adopted. A free-free edge support condition for the specimen under testing produced more precise material damping.

2. Theoretical

A. Determination of basic damping loss factors in partially delaminated composites

A.1 Experimental approach

Three kinds of sample coupons (i. e. 0°, 45°, 90°) were made to directly evaluate η_{dL}, η_{dT} and η_{dLT} as funtions of delamination areas, as shown in Fig. 3. The proposed experimental technique is a straightforward approach to the determine variations in basic damping properties induced by partial delamination.

A.2 Analytical approach

Delamination growth in a laminated composite due to out-of-plane stresses is accompanied with the stiffness loss. In order to analyze stiffness loss due to delamination cracks, Aboudi's theory (Aboudi, 1987) was utilized with the assumption that the same sized and shaped delaminated strips exist symmetrically at both edges of the composite laminate, as shown in Fig. 1. Effective Young's modulus and shear modulus in partially delaminated composite coupon with various delamination sizes must be determined. For a simple approximation, we assumed that the fiber exposed due to free-edge delamination in the

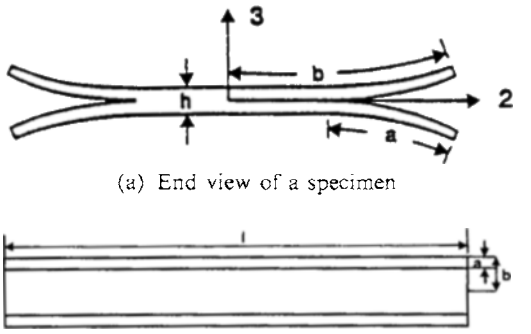

(a) End view of a specimen

(b) Top view of a specimen

Fig. 1 Delamination specimen geometry

composites does not get damaged but the matrix resin does. Under this assumption the fiber modulus does not change. By calculating the stiffness reduction of the matrix resin from Aboudi's theory we can theoretically estimate the damping loss factor in a composite containing a delamination crack from the following formulae.

Based upon the strain energy method and the law of energy conservation, the loss factor of a fiber reinforced composite was obtained by summing up the energy dissipation associated with both the fiber and the matrix and then dividing the sum by the total energy stored in the composite :

$$\eta_t = \frac{\eta_f W_{0f} V_f + \eta_m W_{0m} V_m}{W_{ot}} \tag{1}$$

The loss factor of a cracked matrix resin was determined by adding the energy dissipation associated with both the crack and the matrix. Fundamental loss factor of the matrix resin with delamination cracks can be deduced from Eq. (1) as follows :

$$\eta_{dm} = \eta_m (1 - V_f) \frac{E_m}{E_{dm}} \tag{2}$$

where,

η_{dm} : the loss factor of matrix induced by delamination,

η_m : the loss factor of undamaged matrix,

E_m : Young's modulus of undamaged matrix,

E_{dm} : Young's modulus of matrix induced by delamination,

V_f : the delamination crack volume fraction ($\simeq 0$).

Since the matrix resin is an isotropic material, it is not necessary to introduce a composite manufacturing parameter. The above formula can be regarded as a lower bound of fundamental loss factor because the Coulomb frictional energy due to slip between the laminae in delaminated regions has not been considered.

The basic axial loss factor (η_{dL}) of a unidirectional composite induced by delamination is represented by :

$$\eta_{dL}=\frac{\eta_{dm}V_m}{V_m+V_f\left(\frac{E_{Lf}}{E_{dm}}\right)^{\alpha}} \tag{3}$$

where,

η_{dm} : the loss factor of the matrix containing a delamination crack,

η_{dL} : the axial loss factor of a unidirectional composite with delamination,

V_f : the fiber volume fraction $(1-V_m)$,

E_{dm} : Young's modulus of the matrix with delamination,

α : the composite manufacturing parameter under axial loading determined from undamaged composites.

The basic transverse loss factor (η_{dT}) in a unidirectional composite due to delamination cracks can be evaluated by selecting a suitable E_{dm} for free-edge delamination and by modifying it based on the elastic-viscoelastic correspondence principle and the rule-of-mixtures law as follows :

$$\eta_{dT}=\eta_{dm}-\frac{\eta_{dm}V_f}{V_f+V_m\left(\frac{E_{Tf}}{E_{dm}}\right)^{\zeta}} \tag{4}$$

where,

E_{dm} : effective Young's modulus of the matrix induced by delamination,

η_{dT} : the transverse damping loss factor of a unidirectional composite induced by delamination,

ζ : the composite manufacturing parameter under transverse loading determined from undamaged composites.

The basic longitudinal shear loss factor (η_{dLT}) induced by delamination is expressed as

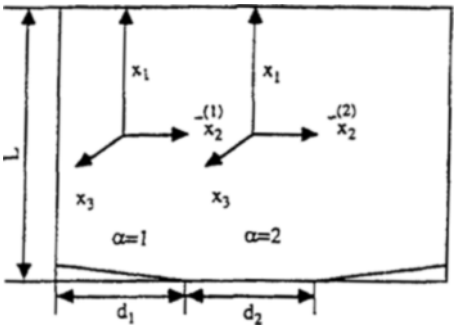

Fig. 2 Model for equivalent moduli evaluation of matrix with symmetric crack

$$\eta_{dLT}=\frac{\eta_{dm}(1-V_f)[G+1)^{(2+\beta)}+V_f(G-1)^{(2+\beta)}]}{[G^{(1+\beta)}(1+V_f)+1-V_f][G^{(1+\beta)}(1-V_f)+1+V_f]} \tag{5}$$

where,

$G=G_f/G_{dm}$,

G_f : the longitudinal shear modulus of fiber,

G_{dm} : the shear modulus of matrix with delamination,

β : the composite manufacturing parameter under shear loading determined from undamaged composites.

The longitudinal shear basic loss factor induced by delamination can be obtained by substituting the equivalent effective shear modulus of the matrix with delamination cracks into Eq. (5). The basic loss factors of partially delaminated composites can be experimentally evaluated and compared to those theoretically calculated.

B. Evaluation of effective modulus for a matrix with partially delaminated cracks

In order to analyze the effective moduli of symmetric cracks in a solid, we considered an infinite elastic solid containing a doubly periodic rectangular array of slit-like cracks subjected to a uniform stress (Aboudi, 1987 ; Delameter et. al., 1975). On the basis of a unit cell as shown in Fig. (2), the displacement vector is expanded to a second order polynomial in terms of the distance from the centerline for derivation of effective moduli.

B. 1. Calculation of effective Young's modulus (Aboudi, 1987)

To solve the internal strain energy in the unit cell, we used the equilibrium equation associated with the continuity conditions for the displacement and stress. It gave us system equations in terms of the elastic field variables. From these system equations, we can determine the field variables in a second order Legendre polynomial. The elastic strain energy in the unit cell region may be expressed by

$$W=\int_{-L/2}^{L/2}\int_{-d1/2}^{d1/2} W_0^{(1)}dx_1\overline{dx}_2^{(1)} + \int_{-L/2}^{L/2}\int_{-d2/2}^{d2/2} W_0^{(2)}dx_1\overline{dx}_2^{(2)} \tag{6}$$

where $W_0^{(\alpha)}$ was derived as follows;

$$\begin{aligned} W_0^{(\alpha)} &= \frac{1}{2}\sigma_{ij}^{(\alpha)}\varepsilon_{ij}^{(\alpha)} \\ &= \left[A_{11}^{(\alpha)}\frac{\partial}{\partial x_1}U^{(\alpha)} + A_{12}^{(\alpha)}\Psi^{(\alpha)}\right]\frac{\partial}{\partial x_1}U^{(\alpha)} \\ &\quad + \left[A_{12}^{(\alpha)}\frac{\partial}{\partial x_1}U^{(\alpha)} + A_{22}^{(\alpha)}\Psi^{(\alpha)}\right]\Psi^{(\alpha)} \\ &\quad + \frac{d_\alpha^2}{12}c_{66}^{(\alpha)}\left[\frac{\partial}{\partial x_1}\Psi^{(\alpha)} + 3\Phi^{(\alpha)}\right]^2 \\ &\quad + \frac{d_\alpha^4}{80}A_{11}^{(\alpha)}\left[\frac{\partial}{\partial x_1}\Phi^{(\alpha)}\right]^2 \end{aligned} \tag{7}$$

where,

A_{IJ} is effective moduli, and

$U^{(\alpha)}$, $\Psi^{(\alpha)}$ and $\Phi^{(\alpha)}$ are the coefficients of the second order Legendre polynomial for displacements determined from the system equations.

The effective mechanical behavior of the cracked solid can be expressed by

$$\overline{\sigma}_{11}=A_{11}^*\overline{\varepsilon}_{11}+A_{12}^*\overline{\varepsilon}_{22} \tag{8}$$

$$\overline{\sigma}_{12}=A_{12}^*\overline{\varepsilon}_{11}+A_{22}^*\overline{\varepsilon}_{22} \tag{9}$$

where A_{IJ}^* represents the equivalent effective moduli.

With the unit displacement at the boundary, the average strain can be represented as $\overline{\varepsilon}_{11}=1/L$.

The average strain, $\overline{\varepsilon}_{22}$ can be expressed by

$$\begin{aligned} \overline{\varepsilon}_{22} &= \frac{d_1\varepsilon_{22}^{(1)}+d_2\varepsilon_{22}^{(2)}}{(d_1+d_2)} \\ &= \frac{d_1\Psi^{(1)}+d_2\Psi^{(2)}}{(d_1+d_2)}=0 \end{aligned} \tag{10}$$

Therefore, under opening loading(Mode I) condition, we found the following relation in a unit cell:

$$\frac{1}{2}\overline{\varepsilon}_{11}^2A_{11}^*(d_1+d_2)L=W \tag{11}$$

from which A_{11}^*(equivalent effective modulus) can be determined.

In the crack direction, the Poisson's ratio, ν_{21} of the uncracked solid body is unaffected by cracks, such that

$$A_{12}^*=\nu_{21}A_{11}^* \tag{12}$$

Also, Young's modulus, E_2, of uncracked solid body is not influenced by cracks:

$$E_2=\frac{A_{11}^*A_{22}^*-(A_{12}^*)^2}{A_{11}^*} \tag{13}$$

from which A_{22}^* can be determined.

Finally, the effective Young's modulus, E_1^*, of cracked solid body in the x_1-direction can be obtained from

$$E_1^*=\frac{A_{11}^*A_{22}^*-(A_{12}^*)^2}{A_{22}^*} \tag{14}$$

Thus, the longitudinal basic damping loss factor at a particular free-edge delamination area can be computed by substituting the equivalent effective Young's modulus of a matrix with symmetric delamination cracks into Eqs. (2), (3) and (4).

B. 2. Calculation of effective shear modulus (Aboudi, 1987)

The theoretical treatment of shear modulus is the same as that of Young's modulus. The solid is subjected to a stress distribution at infinity resulting in a state of antiplane strain. The elastic strain energy due to shear loading in the representative model is then

$$W=\int_{-L/2}^{L/2}\int_{-d1/2}^{d1/2} W_0^{(1)}dx_1d\bar{x}_2^{(1)} + \int_{-L/2}^{L/2}\int_{-d2/2}^{d2/2} W_0^{(2)}dx_1d\bar{x}_2^{(2)} \tag{15}$$

where $W_0^{(\alpha)}$ is the strain energy density which was expressed by:

$$\begin{aligned} W_0^{(\alpha)} &= \frac{1}{2}\sigma_{ij}^{(\alpha)}\varepsilon_{ij}^{(\alpha)} \\ &= c_{66}^{(\alpha)}\left[Y^{(\alpha)}+\frac{\partial}{\partial x_1}V^{(\alpha)}\right]+\frac{d^2\alpha}{12}\left[A_{11}^{(\alpha)}\frac{\partial}{\partial x_1}Y^{(\alpha)} \right. \\ &\quad \left. +3A_{13}^{(\alpha)}Z^{(\alpha)}\right]\frac{\partial}{\partial x_1}Y^{(\alpha)}+\frac{d_\alpha^2}{4}\left[A_{13}^{(\alpha)}\frac{\partial}{\partial x_1}Y^{(\alpha)}\right. \end{aligned}$$

$$+3A_{33}^{(\alpha)}Z^{(\alpha)}\Big]Z^{(\alpha)}+\frac{d_\alpha^4}{80}c_{66}^{(\alpha)}\Big[\frac{\partial}{\partial x_1}Z^{(\alpha)}\Big]^2 \quad (16)$$

where,

c_{ij} is the general Hooke's constants,

A_{ij} is the effective moduli,

$Y^{(\alpha)}$, $V^{(\alpha)}$ and $Z^{(\alpha)}$ are the coefficients of the second order Legendre polynomial for displacements.

The equivalent effective shear modulus G_{12}^* was found by using sliding mode II condition :

$$2\bar{\varepsilon}_{12}^2 G_{12}^*(d_1+d_2)L=W \quad (17)$$

where, $\bar{\varepsilon}_{12}=\frac{1}{2L}$.

Thus, the longitudinal shear loss factor at a free-edge delamination area can be computed by substituting the equivalent effective shear modulus (G_{12}^*) of a matrix with symmetric delamination cracks into Eq. (5).

C. Damping prediction in partially delaminated composites

We predicted the loss factor in a partially delaminated composite of any stacking sequence by utilizing their basic damping properties. From Adams and Ni (Ni and Adams, 1984), the strain energy dissipation which is subjected to bending in the partially delaminated composite beam is divided into three parts related to inplane stresses (σ_x, σ_y and σ_{xy}) in the fiber coordinate system.

Simply,

$$\Delta W_d=\Delta W_{dx}+\Delta W_{dy}+\Delta W_{dx} \quad (18)$$

The strain energy dissipation about σx is written as follows :

$$\begin{aligned}\Delta W_{dx}&=\int_0^l 2\int_0^{h/2}\pi\eta_{dL}\sigma_x\varepsilon_x dzdx\\&=2\pi\eta_{dL}\int_0^l\int_0^{h/2}\sigma_x\varepsilon_x dzdx\\&=\frac{2\pi\eta_{dL}}{I^{*2}}\int_0^{h/2}m^2(Q_{11}d_{11}^*+Q_{12}d_{12}^*+Q_{16}d_{16}^*)\cdot\\&\quad(m^2d_{11}^*+mnd_{16}^*)z^2dz\int_0^l M_1^2dx\end{aligned} \quad (19)$$

where,

l is the length of beam, h is the thickness of beam,

$$\eta_{dL}=\frac{\eta_m V_m}{V_m+V_f\left(\frac{E_{Lf}}{E_{dm}}\right)^\alpha}$$

is the axial loss factor of partially delaminated 0° unidirectional composites,

η_{dm} is the matrix resin loss factor induced by partial delamination,

M_1 is the bending moment in the cantilever beam,

α is the curve fitting parameter,

I^* is the normalized moment of inertia,

d_{11}^* is the normalized flexural compliance along the axis.

Similarly, ΔW_{dy} and ΔW_{dxy} can be evaluated as follows :

$$\begin{aligned}\Delta W_{dy}=&\frac{2\pi\eta_{dT}}{I^{*2}}\int_0^{h/2}n^2(Q_{11}d_{11}^*+Q_{12}d_{12}^*+Q_{12}d_{16}^*)\cdot\\&(n^2d_{11}^*-mnd_{16}^*)z^2dz\int_0^l M_1^2dx\end{aligned} \quad (20)$$

$$\begin{aligned}\Delta W_{dxy}=&\frac{2\pi\eta_{dLT}}{I^{*2}}\int_0^{h/2}mn(Q_{11}d_{11}^*\\&+Q_{12}d_{12}^*+Q_{16}d_{16}^*)(2mnd_1^*)\\&-(m^2-n^2)d_{16}^*)z^2dz\int_0^l M_1^2dx\end{aligned} \quad (21)$$

And the bending strain energy of the beam is

$$W_b=\int_0^l M_1x_1dx=\frac{d_{11}^*}{I^*}\int_0^l M_1^2dx \quad (22)$$

The total loss factor (η_{dov}) in partially delaminated composites is also described as :

$$\psi_{dov}=\frac{\sum\Delta W_d}{\sum W}=\frac{\Delta W_{dx}+\Delta W_{dy}+\Delta W_{dxy}}{W_b} \quad (23)$$

where,

$\psi_{dov}=2\pi\eta_{dov}$ is the specific damping capacity in partially delaminated composites,

η_{dov} is the overall loss factor in partially delaminated composites.

3. Experiments

Basic damping properties should be determined through experimental work together with theoretical modeling. Theoretical values of basic damping properties due to partial delamination can be evaluated using the modified rule of mixtures and Hashin's approach. In order to verify the theoretical values, the experimental work was carried out. At first, three kinds of sample coupons were made for evaluating η_{dL}, η_{dT} and η_{dLT} as funtions of

delamination areas, as shown in Fig. 3. This experimental technique has the advantage that it is a very straightforward approach to determine variations of basic damping properties induced by partial delamination. The experimental results are presented and compared with theoretical basic damping properties. Consequently, we measured the damping loss factors of various composites with different stacking sequences experimentally and predicted these loss factors theoretically by utilizing their basic damping properties.

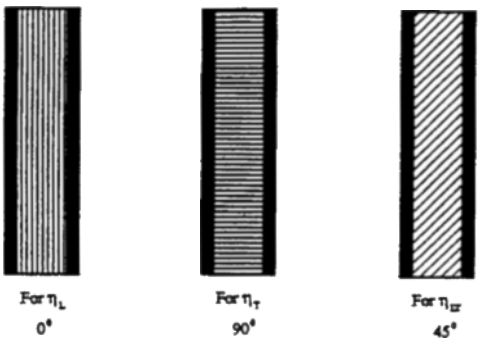

Fig. 3 Specimens for measuring basic damping properties of laminated composites influenced by partial delamination

3.1 Experimental setup

The damping from the supports of the specimen and other dampings, such as that from the connecting cables must be avoided since our main aim was to measure the damping of a graphite epoxy composite. In the damping measurement of a beam, the best way to avoid damping from supports is to use a free-free support condition for the beam and excite it at its center through an impedance head mounted on a shaker. Figure 4. shows a schematic of the experimental setup for measuring the damping of partially delaminated

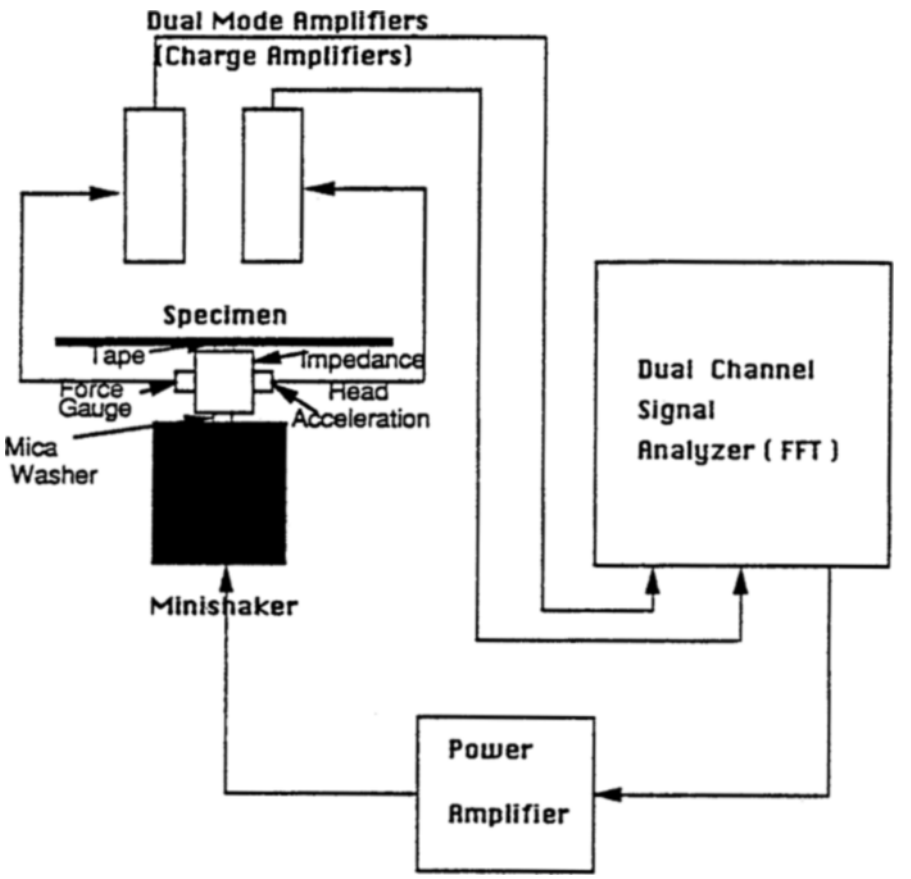

Fig. 4 Improved Experimental Setup for Measurement of Material Damping

composite beam specimens. The beam specimen was excited by means of an electrodynamic exciter driven by a random noise generator (Suarez et al., 1984). The exciter was a minishaker (Bruel & Kjaer 4810). The double cantilever support condition for the specimen was set up by mounting the specimen at its center directly on the impedance head using 1mm-width strip of a double-sided adhesive tape.

The impedance head (Bruel & Kjaer 8000) was mounted on the exciter and it directly measured the acceleration response and the input force of the beam specimen. The input force signal to the beam and the output acceleration signal from it were fed through two charge amplifiers to a Dual Channel Signal Analyzer (Bruel & Kjaer 2032). The Dual Channel Signal Analyzer was used to determine the frequency response function, $\frac{A}{j\omega F} = \frac{V}{F}$(Mobility), from the force and acceleration signals of the impedance head connected to the specimen. The damping value for each of the specimens was measured by using the typical half power bandwidth methods in a zoom mode with narrow frequency span of the frequency response of the specimen.

3.2 Improving the mounting of beams

The mounting of beam specimens under testing played an important role in damping measurements. Hence, considerable time and effort was spent to select the best mounting method. Supporting a beam at its center prevents excessive damping from the supports as in the case of a cantilevered or a simply supported beam. Unfortunately, the center point is the antinode of the odd mode vibration of the beam, and a load at the antinode will produce the largest impact response. If the load is a mass, it will only lower the resonance frequencies ; if it is a resistance, it will not only lower the resonance frequencies but also increase the damping(Morse and Ingrad, 1968). After extensive trials with wax, stud, glue and tape, the double sided adhesive thin tape was chosen to mount the specimens. Wax is not ideal, because a mounting with less wax tends to be too loose while the specimen is vibrating, and if too much wax is used, the measured damping ratio will be very high. Although the stud mounting is stable, it tends to decrease the resonance frequencies and increase the damping ratio value significantly. Glue mounting is also stable, but the surface area of contact between the beam and the impedance head is often too large, hence the measured damping ratio value will be higher than that of the specimen under testing.

In order to get a stable and minimally damped support for making damping measurements, a narrow piece of carpet tape about 1mm in width was stuck at the center of the beam perpendicular to the length of the beam. Since the tape was very thin, it was necessary to balance the beam. This was done by ensuring that the gap between the beam and the impedance head on either side of the tape mounting was the same.

3.3 Further check of the measured results

In order to ensure reliable experimental results, a further check was always conducted during the measurement procedure. The signal to noise ratio and coherence between the two channels were observed for each measurement. Acceptable experimental conditions were found to be a signal to noise ratio of over 20 dB, a coherence of over 0.91, and a very small difference between the frequency responses H2 and H1 measured by the B&K Analyzer. At the same time, the repeatability of several successive results was also tested. It was found that as the signal to noise ratio, coherence and the value of the damping ratio decreased, the difference between H2 and H1 and the resonance peak increased quickly. The reason was most often found to be slack mounting of the beam.

3.4 Specimen fabrication

Three kinds of partially delaminated 3M graphite/epoxy composites were investigated in this damping study. All the composite panels were manufactured in the compression molding machine according to manufacturer's recommended cure cycle. All panels were fabricated from 8 plies of 3M graphite/epoxy prepreg. The layup

was subjected to compression molding at 80 PSI and 80 ℃ for 2 hours. After compression molding, it was also subjected to post curing at 150 ℃ for 2 hours. The partial delaminations at the specimen midsurface were embedded by inserting two layers of Kapton film. Furthermore, after cutting identical composite beam specimens, partial delamination cracks were also made by scoring with a thin razor blade. The fiber volume fraction of the composite material used in this study was about 55 % in all specimens. The beam specimens of dimensions $7\times1.0\times0.042$ inch were machined from these fabricated plates. It should be noted that when specimen were trimmed, there existed little difference(±0.5 inch) among their lengths.

4. Results and Discussion

The numerical and experimental results which were correlated between damping loss factor and delamination sizes were presented in Figs. 5～10. The curve fitting parameters, based upon the experimental results for the basic loss factors of these undamaged laminated composites, were used to evaluate loss factors for 8-ply 3-M Graphite/Epoxy partially delaminated composites. These parameters can exhibit the influence of fiber/matrix interface and fiber on the composite material damping. The variation of damping with fiber orientation in delaminated composites follows a trend similar to that in laminated composites (Figs. 8～10). The loss factor is significantly dependent on delamination sizes and fiber orientation in off-axis partially delaminated unidirectional composites. The loss factor can be enhan-

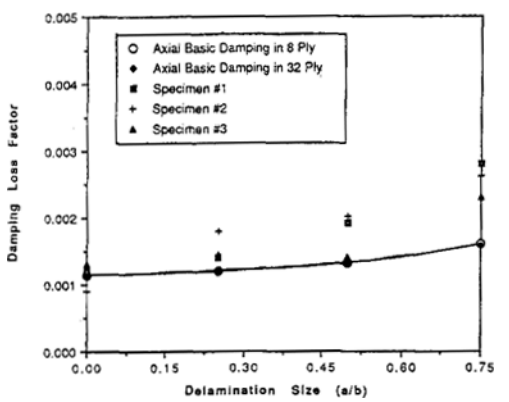

Fig. 5 Variation of axial basic loss factor with various delamination sizes

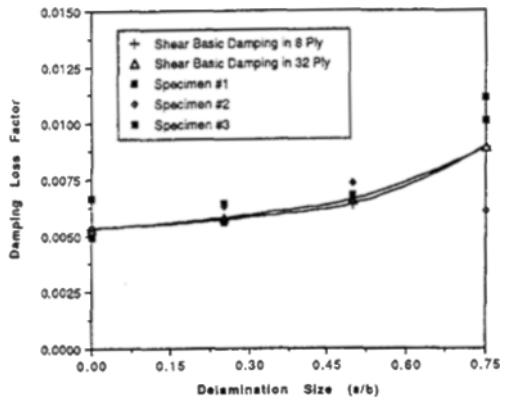

Fig. 6 Variation of in-plane shear loss factor with various delamination sizes

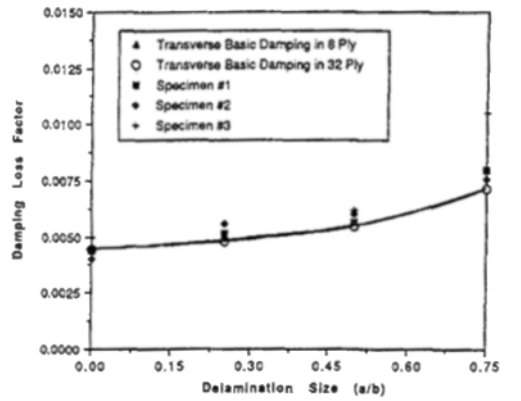

Fig. 7 Variation of transverse basic loss factor with various delamination sizes

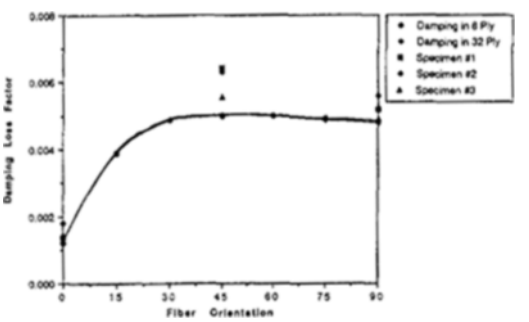

Fig. 8 Variation of loss factor as a function of fiber orientation in a/b=0.25 partial delamination size of 3M Gr/Ep laminate

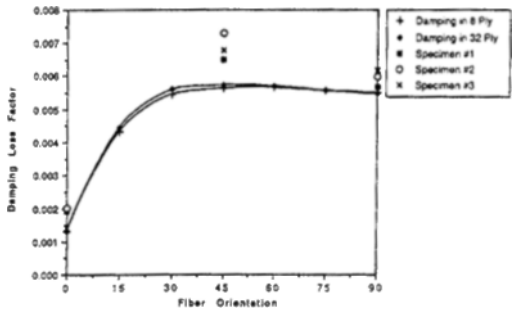

Fig. 9 Variation of loss factor as a function of fiber orientation in a/b=0.5 partial delamination size of 3M Gr/Ep laminate

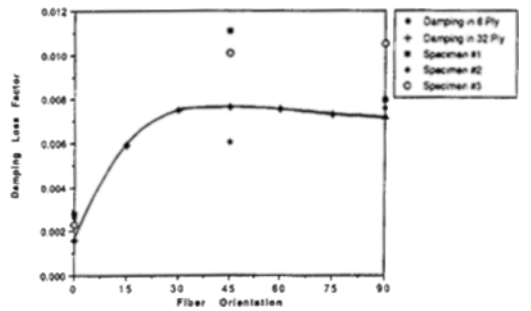

Fig. 10 Variation of loss factor as a function of fiber orientation in a/b=0.75 partial delamination size of 3M Gr/Ep laminate

ced by increasing delamination area in laminated composites. Theoretical expressions for damping appear to underestimate the measured values as shown in Figs. 5~10. The discrepancies may mainly be attributed to the Coulomb slipping mechanism between delaminated areas. As the delamination size increases, the η_L and η_T values of the 8-ply specimens were slightly more influenced than those of the 32-ply specimens (Figs. 5 and 7). One possible reason is that a thin specimen has higher stiffness reduction than thick one due to delamination. For η_{LT}, as shown in Fig. 6, the damping behavior is just opposite to that for η_L and η_T.

In the improved free-free support damping measurement method, it is difficult to obtain the same damping value repeatedly. Each time the specimen is mounted on the impedance head, the damping value is slightly different. Even though the repeatability is low, true material damping values could be measured owing to significantly reduced extraneous energy dissipation caused by boundary conditions. Damping was strongly influenced by the curing cycle (i. e. the degree of crosslinking) of the specimen, the type of impedance head used, the nature of the mounting materials between the specimen and impedance head, and the mounting material size and thickness. Particularly, in the partially delaminated composites, it appears that damping is highly affected by the amplitude of force. In order to minimize these complicating effects, experimental works were performed in a consistent manner during evaluation of the damping in partially delaminated graphite/epoxy composites.

5. Conclusions

(1) A model for predicting the damping in partially delaminated composites has been developed based upon the Adams and Ni's work and the obtained basic damping loss factors.

(2) Although some differences exist between the theoretical and experimental values, this theoretical model provides the lower bound solution of damping in partially delaminated composites.

(3) By using the improved experimental method. more accurate material damping can be measured owing to significantly reduced extraneous energy dissipation from boundary conditions.

(4) The variation of damping with fiber orientation in partially delaminated composites exhibited a similar trend to that in laminated composites.

(5) It was quantitatively confirmed that the damping loss factor increases gradually with increasing delamination size.

Acknowledgments

The support for this project was provided by the NSF/Alabama EPSCOR program to which we are grateful.

References

Hashin, Z., 1970, "Complex Moduli of Vis-

coelastic Composites : II. Fiber Reinforced Materials," *Int. J. solids and struc.*, Vol. 6 pp. 797 ~807.

Adams, R. D., 1987 "Damping Properties Analysis of Composites," *Engineering Materials Handbook*, Composites, Vol. 1, pp. 206~217, ASM.

Reifsnider, K. L., Henneke, E. G. and Stinchcomb, W. W., 1979, "Defect Property Relationships in Composite Materials," AFML-TR-81, Part IV, *Air Force Materials Laboratory*.

Highsmith, A. L. and Reifsnider, K. L., 1982, "Stiffness Reduction Mechanisms in Composite Laminates," in Damage in Composite Materials, ASTM STP 775, *American Society for Testing and Materials*, Philadelphia, PA, pp. 103~117.

O'Brien, T. K., 1982, "Characterization of Delamination Onset and Growth in a Composite Laminate," Damage in Composite Materials, ASTM STP 775, K. L. Reifsnider, Ed., *American Society for Testing and Materials*, pp. 140~167.

Aboudi, J., 1987, "Stiffness Reduction of Cracked Solids," *Engineering Fracture Mechanics*, Vol. 26, No. 5, pp. 637~650.

Delameter W. R., Herrmann G. and Barnett, D. M.," 1975, Weakening of an Elastic Solid by a Rectangular Array of Cracks," *Journal of Applied Mechanics*, pp. 74~80.

Ni, R. G. and Adams, R. D., 1984, "The Damping and Dynamic Moduli of Symmetric Laminated Composite Beams Theoretrical and Experimental Results," *J. Comp. Matls*, Vol. 18, p, 104.

Crocker, M. J., Raju, P. K., Rao, M. D. and Yan, Xinche, 1984, "Measurement of Damping of Graphite Epoxy Materials & Structural Joints," *NASA New Technology Report* MFS-27228.

Suarez, S. A., Gibson, R. F. and Deobold, L. R., 1984, "Random and Impulse Techniques for Measurements of Damping in Composite Materials," *Experimental Techniques*, Vol. 8, No. 10, pp. 19~24.

Morse, P. M. and Ingrad, K. U., 1968, *Theoretical Acoustics*, McGraw- Hill.